Mechanical response of freestanding Au nanopillars under compression

Luis A. Zepeda-Ruiz,[a] Babak Sadigh, Juergen Biener, Andrea M. Hodge, and Alex V. Hamza
Chemistry, Materials, and Life Sciences Directorate, Lawrence Livermore National Laboratory, Livermore, California 94550

(Received 4 June 2007; accepted 10 August 2007; published online 6 September 2007)

We employ molecular dynamics simulations of defect-free nanopillars with realistic cylindrical geometries to obtain an atomic-level picture of their deformation behavior under compression. We find that dislocations are nucleated in the two outermost surface layers. Furthermore, plastic yield depends crucially on the particular arrangement of steps and facets at the surface of the nanopillars. We show that different facet orientations can differ dramatically in their response to external stresses. Freestanding nanopillars exhibit a highly nonuniform distribution of stresses along their height. This causes an elastic deformation that leads to a barrel-like shape attained by the nanopillars under compression. The stress concentration at the center of the pillars due to barreling causes dislocations to preferentially nucleate in this region. © *2007 American Institute of Physics*.
[DOI: 10.1063/1.2778761]

Size-scale effects in plasticity have recently attracted much interest as the mechanical properties of nanostructured materials are of great technological importance. Recently, size-scale effects in systems where the characteristic length scale is given by the sample dimension rather than an internal length scale (such as the grain size in nanocrystalline materials[1,2]) have been the subject of considerable interest.[3–13] This sample size effect can qualitatively be understood in terms of the "nucleation starvation" model developed by Greer *et al.*[6] which results in the general observation that smaller is stronger. As the mechanical behavior of a material relies on defect generation/interaction, one must take into account cases where no internal dislocation sources can be accommodated and surface effects become important. Toward this end, molecular dynamics simulations have been performed on a variety of systems.[14–23] Although these studies provide insight into plastic deformation mechanisms, a clear understanding of this effect is still missing. This is mainly because these studies were performed on systems with sizes and shapes different from those used in experiments.

In this letter, we present molecular dynamics (MD) simulations of the mechanical response of ideal defect-free Au pillars under compressive deformation to investigate yield mechanisms. Our study is based on [001]-oriented nanopillars with realistic cylindrical geometries with aspect ratios of 1:2 in diameter:height. The largest pillar size included here is 20:40 nm, containing $\sim 1 \times 10^6$ atoms. We have worked with highly symmetric nanopillars whose surfaces are covered by steps that delimit mainly two types of facets: {100} and {110}. Because of this, the whole surface can be represented by only three types of atoms: {110} terrace atoms, {100} terrace atoms, and step edge atoms. Note that nanopillars of any size can be constructed such that the number of terraces and surface steps are kept fixed and only the widths of the terraces increase with increasing system size.

Our MD simulations were performed using the LAMMPS code[24] with an embedded atom method to describe Au properties.[25] In order to simulate a freestanding nanopillar we used free boundary conditions in all three directions. Along the [001] direction (z direction), we constrained the motion of the atoms in the top/bottom two layers. The atoms in each of the four layers were forced to be coplanar during compression, allowing only motion along the [100] and [010] directions (x and y directions, respectively). Uniaxial compression was performed along the [001] orientation by rescaling the height of the pillars at a strain rate of 2×10^8 s^{-1}. Three different temperatures were used in our study: 0, 30, and 300 K. Initially, the nanopillars had to be equilibrated to zero overall pressure for several thousand simulation steps since they were not in an equilibrium state due to the presence of surface stresses. During equilibration, the pillars contract along both the radial and axial directions to balance the tensile stresses produced by the surfaces. This results in a compressive state of stress in the interior of the nanopillars, similar to the effect seen for small Au nanowires.[17,18] Upon analyzing the variation of the atomic-level stresses as a function of the distance from the center of the nanopillars, we find that apart from a few outer layers that constitute the surface region, the interior can be modeled as a uniform bulk system under an external compressive load. We estimate the thickness of the surface layer to be $\sim$4.5 nm.

Figure 1(a) shows the stress-strain curves obtained by applying a 10% compressive deformation to a 20:40 nm freestanding nanopillar at different temperatures. We observe in all cases a linear elastic response for small deformations, followed by a nonlinear elastic regime until the stress reaches a maximum value. At this point of deformation, the system will not be able to sustain any more stress and will start yielding. The yield mechanism is initially purely elastic and thus reversible. However, upon further compression, irreversible plastic deformation occurs by nucleation of $\langle 112 \rangle \{111\}$ partial dislocations at the surface of the nanopillars. With increasing temperature, the systems soften elastically and consequently yield at lower compressions.

We have extensively studied the details of the atomistic processes at the onset of plasticity. In fact, we find that these

[a]Electronic mail: zepedaruiz1@llnl.gov

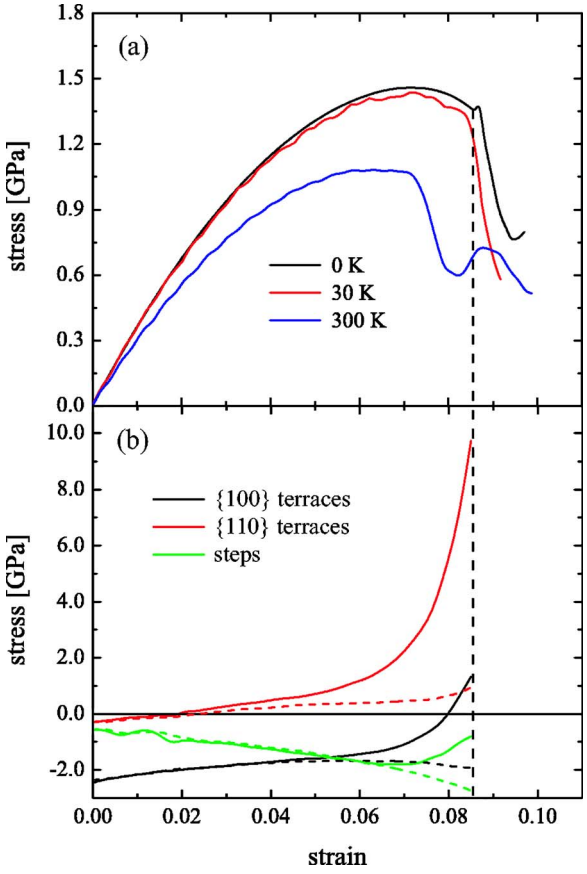

FIG. 1. (Color online) (a) Compressive stress-strain curves for a 20:40 nm freestanding nanopillar at different temperatures. (b) Stress-strain curves for the three types of atoms at the surface of the same nanopillar at 0 K. The solid lines correspond to the surface atoms in the middle region of the cylinder. The dashed curves represent all the surface atoms throughout the entire height of the cylinder. Negative stresses indicate tension.

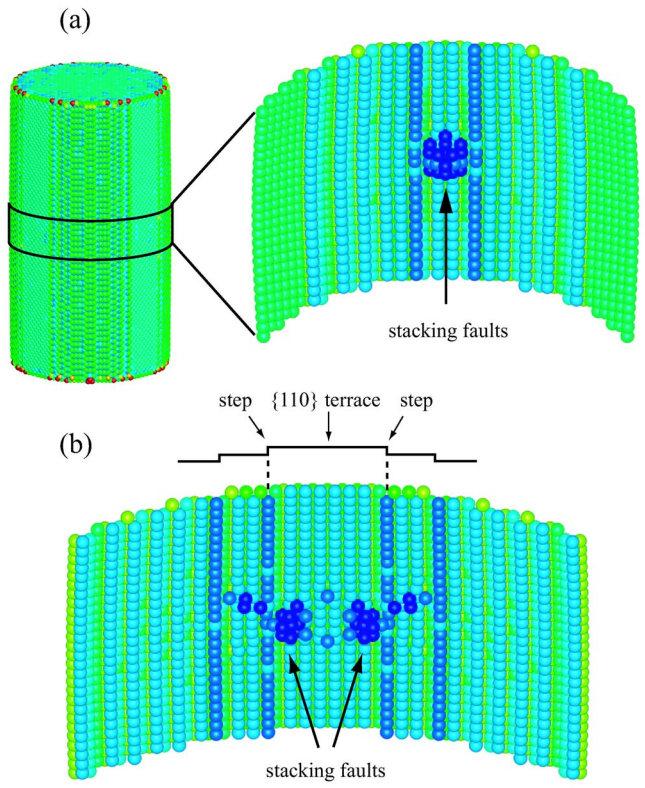

FIG. 2. (Color online) Nucleation of partial dislocations near the step edges for a (a) 10:20 nanopillar and (b) 20:40 nm nanopillar at 0 K.

processes are highly sensitive to the arrangement of the specific facets on the surface of the cylinders and that different facet orientations can differ dramatically in their response to external stress. Consequently, the onset of plasticity is dictated by how strong each specific surface feature couples to the applied stress. Furthermore, for freestanding nanopillars we find that plasticity is always initiated in their middle region. This is due to a nonuniform stress distribution along the height of the cylinders leading to concentration of stress in the center of such nanopillars. This effect is absent when periodic boundary conditions are enforced, since for such systems the stress is uniform throughout the height of the cylinders.

Figure 1(b) shows the stress-strain curves for the three surface atom types mentioned earlier. Solid curves represent the elastic behavior of the surface atoms located in a 2 nm thick region in the middle of the pillar where dislocations nucleate. Dashed curves show the same quantities averaged throughout the entire height of the cylinder. We observe that all the surface atoms are initially under tensile stress (negative values). However, upon compression, the {110} terrace atoms in the center of the cylinder couple strongly to the applied stress and become increasingly compressed. It is important to emphasize that for the specific case of [001]-oriented Au nanopillars chosen for this study, the total stress in Fig. 1(a) decreases beyond the elastic yield point prior to plasticity. This means that in our case the total stress of the system is not necessarily correlated with the onset of plasticity. In addition, the surface stress of the (110) terraces increases monotonically toward the singular point where plasticity is initiated. Hence, the driving force for dislocation nucleation is the compressive stress at the {110} facets. To further illustrate this point, we show in Fig. 2 the configurations of the middle regions of two nanopillars of different sizes right at the onset of plasticity. We observe that dislocations are nucleated next to the outermost surface layer of the {110} facets close to a step edge. Dislocation are visualized by removing all atoms with perfect fcc neighborhoods according to a centrosymmetry deviation filter.[26]

Above, we have shown that the surface stress in the middle region of the freestanding cylinders [solid lines in Fig. 1(b)] can deviate significantly from the average [dashed lines in Fig. 1(b)], specially during compression. This nonuniform distribution of stresses is a result of the reduction of elastic energy in the presence of surfaces and causes the system to exhibit a barrel-like shape. Barreling causes the stress/deformation to be highest around the middle region of the cylinders. Figure 3 shows the vertical profile of a 10:20 nm nanopillar at different compressive deformations. Elastic deformation causes the barrel shape to become progressively more pronounced. Note that even in the absence of external stresses, a nonzero barreling is attained by the nanopillar due to the compressive stresses exerted by the top and bottom surfaces.

As mentioned earlier, in freestanding systems, partial dislocations always nucleate in the middle region of the nanopillars (see Fig. 2). These dislocations propagate through the bulk of the system along the {111} planes (the natural glide planes for fcc) leaving behind a series of stacking faults that traverse the entire system. Once the stacking

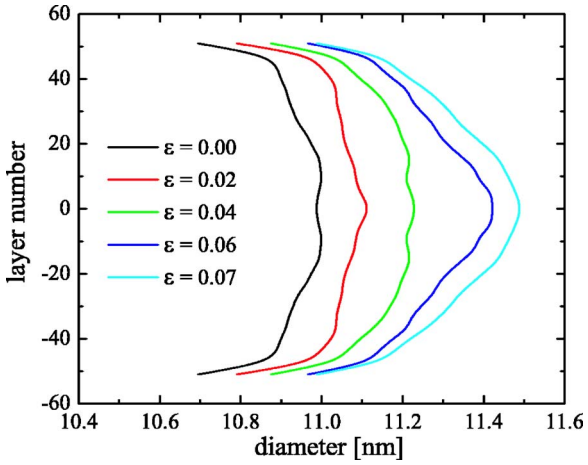

FIG. 3. (Color online) Shape evolution as a function of deformation for a 10:20 nm pillar.

faults reach the opposite side, the cylinder slips and a sudden reduction in stress is observed in the stress-strain curves. As deformation proceeds, twinning and secondary nucleation events are observed. Figures 4(a) and 4(b) show the final states of a 10:20 nm pillar after 10% compression at 0 and 30 K, respectively. While both temperature cases show the presence of stacking faults, the absence of symmetry breaking in the 0 K calculations preserves the mirror symmetry of the system even after plasticity has taken place [see Figs. 4(a) and 4(b)]. This leads to symmetric dislocation networks that cause extra hardening of the system upon plasticity. Hence, randomization via temperature is necessary to obtain structures resembling those observed during microcompression tests of submicron size pillars (at a different scale) where slip bands are generated by dislocations.[3–7]

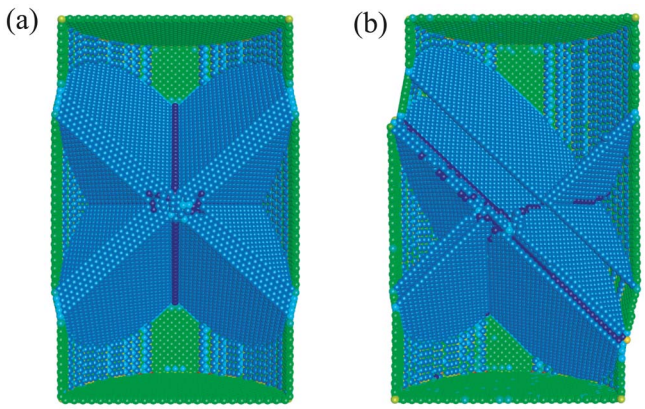

FIG. 4. (Color online) Final state of a 10:20 nm nanopillar after 10% compressive deformation at (b) 0 K and (c) 30 K.

In summary, we have simulated the mechanical response of freestanding Au nanopillars under compressive deformations. We show that the highly nonuniform distribution of surface stresses causes the systems to attain a barrel-like shape that increases upon compression. We find that the onset of plasticity depends on how strong specific surface features couple to the applied stress. Our simulations show that nucleation of surface dislocations happen near the step edges bounding {110} facets.

Fruitful discussions with F. F. Abraham are gratefully acknowledged. This work was performed under the auspices of the U.S. Department of Energy by the University of California, Lawrence Livermore National Laboratory under Contract No. W-7405-Eng-48.

[1] J. Schiøtz and K. W. Jacobsen, Science **301**, 1357 (2003).
[2] J. Schiøtz, Scr. Mater. **51**, 837 (2004).
[3] M. D. Uchic, D. M. Dimiduk, J. N. Florando, and W. D. Nix, Science **305**, 986 (2004).
[4] M. D. Uchic and D. M. Dimiduk, Mater. Sci. Eng., A **400–401**, 268 (2005).
[5] D. M. Dimiduk, M. D. Uchic, and T. A. Parsatharathy, Acta Mater. **53**, 4065 (2005).
[6] J. R. Greer, W. C. Oliver, and W. D. Nix, Acta Mater. **53**, 1821 (2005).
[7] C. A. Volkert and E. T. Lilleodden, Philos. Mag. **86**, 5567 (2006).
[8] B. Wu, A. Heidelberg, and J. J. Boland, Nat. Mater. **4**, 525 (2005).
[9] B. Wu, A. Heidelberg, J. J. Boland, J. E. Sader, X. Sun, and Y. Li, Nano Lett. **6**, 468 (2006).
[10] N. Agrait, G. Rubio, and S. Vieira, Phys. Rev. Lett. **74**, 3995 (1995).
[11] G. Rubio, N. Agrait, and S. Vieira, Phys. Rev. Lett. **76**, 2302 (1996).
[12] G. Rubio, S. R. Bahn, N. Agrait, K. W. Jacobsen, and S. Vieira, Phys. Rev. Lett. **87**, 026101 (2001).
[13] L. T. Ngo, D. Almécija, J. E. Sader, B. Daly, N. Petkov, J. D. Holmes, D. Erts, and J. J. Boland, Nano Lett. **6**, 2964 (2006).
[14] J. Diao, K. Gall, and M. L. Dunn, Nat. Mater. **2**, 656 (2003).
[15] J. Diao, K. Gall, and M. L. Dunn, Phys. Rev. B **70**, 075413 (2004).
[16] J. Diao, K. Gall, and M. L. Dunn, J. Mech. Phys. Solids **52**, 1935 (2004).
[17] J. Diao, K. Gall, and M. L. Dunn, Nano Lett. **4**, 1863 (2004).
[18] J. Diao, K. Gall, M. L. Dunn, and J. A. Zimmerman, Acta Mater. **54**, 643 (2006).
[19] K. Gall, J. Diao, and M. L. Dunn, Nano Lett. **4**, 2431 (2004).
[20] H. S. Park, K. Gall, and J. A. Zimmerman, Phys. Rev. Lett. **95**, 255504 (2005).
[21] H. S. Park and J. A. Zimmerman, Scr. Mater. **54**, 1127 (2006).
[22] B. Hyde, H. D. Espinosa, and D. Farkas, Journal of the Minerals, Metals and Materials Society **57**, 62 (2005).
[23] E. Rabkin, H. S. Nam, and D. J. Srolovitz, Acta Mater. **55**, 2085 (2007).
[24] S. J. Plimpton, J. Comput. Phys. **117**, 1 (1995).
[25] S. M. Foiles, M. I. Baskes, and M. S. Daw, Phys. Rev. B **33**, 7983 (1986).
[26] C. L. Kelchner, S. J. Plimpton, and J. C. Hamilton, Phys. Rev. B **58**, 11085 (1998).